



www.elsevier.com/locate/atmosenv

Determination of domain for diagnostic wind field estimation in Korea

Jin Young Kim^a, Young Sung Ghim^{a,*}, Yong Pyo Kim^a, Donald Dabdub^b

^aGlobal Environmental Research Center, Korea Institute of Science and Technology, P.O. Box 131, Cheongryang, Seoul 130-650, South Korea ^bDepartment of Mechanical and Aerospace Engineering, University of California, Irvine, CA 92697, USA

Received 23 January 1998; received in revised form 5 February 1999; accepted 2 March 1999

Abstract

A diagnostic routine is applied to estimate wind fields for two coastal areas with mountains in Korea. The reliability of the predicted wind fields is assessed by calculating the maximum differences of wind speed and direction between two successive estimations by increasing the size of the estimation domain over the target domain. The differences decrease and stabilize after a critical increment to produce an optimum domain size used to estimate wind fields. Although a larger radius of influence and a larger grid size could increase the stability of convergence, they smooth the predicted wind field and decrease the resolution. The study also reveals that the estimated wind field shows larger differences from the wind field obtained with all stations available in the country, at higher mountains along the boundaries beyond which stations would be added if larger domains are employed. © 1999 Published by Elsevier Science Ltd. All rights reserved.

Keywords: Diagnostic wind field estimation; Sensitivity analysis; Distribution of stations; Boundary topography

1. Introduction

Considerable research effort has been devoted to the problem of generating gridded wind field data for input into air quality models (Seinfeld, 1988; Solomon, 1995). There are two approaches generally followed to generate the wind fields: prognostic and diagnostic approaches (Kumar and Russell, 1996). Prognostic modeling refers to solving the basic governing equations of mass, momentum, energy, and state to obtain the velocity field. Despite gaining more popularity than ever, particularly when observation data are sparse or when the domain is too large to be assessed by other means, prognostic modeling has not been used on a routine basis because of its inherent computational complexity. Diagnostic analysis employs measured data to generate the gridded wind field. It generally requires less computer resources and its procedures are easily incorporated into air quality models. However, a major drawback of the diagnostic ap-

In the diagnostic estimation of wind field, the target domain is usually the same as the air quality modeling domain. Although the objective is to predict the wind field in the target domain, additional measured data outside the target domain are usually employed in the estimation process in order to minimize the boundary effects. Namely, there is a region (A) outside the target domain (D) where measured data are used but wind field is not estimated. In the present study, the region (D + A)that provides measured data is designated as the estimation domain. Wind data are only estimated for the region (D). Employing a large estimation domain is preferable than enlarging the target domain over the area of concern; on the other hand, handling a large number of measured data imposes a computational burden. The main goal of this paper is to develop a method and heuristics to determine the optimum domain size required to predict wind fields in the target domain. That is one that produces reliable results with minimal computational burden. Sensitivities of the predicted wind field in

1352-2310/99/\$- see front matter \odot 1999 Published by Elsevier Science Ltd. All rights reserved. PII: S 1 3 5 2 - 2 3 1 0 (9 9) 0 0 1 7 4 - 0

proach is that the results depend heavily on the quality of measured data as well as on the method selected to perform the diagnostics.

^{*}Corresponding author.

the target domain to the size of the estimation domain are presented in various situations.

2. Methods

2.1. Model

The diagnostic wind field generation routine for the CIT model, an urban airshed model developed at the California Institute of Technology, USA, is employed in this study (Harley et al., 1993). It uses a two step approach to generate wind fields: (1) interpolation of the measured data field to the model grid, and (2) application of variational procedures to minimize field divergence. The first step is accomplished by the following three procedures: triangulation of measured wind data, computation of the wind vector by a weighted average of three vortices of the interpolating triangles, and adjustment of the wind vectors to account for local terrain features. The second step is comprised of reducing flow divergence by filtering the interpolated data with nonlinear filter and adjusting the wind components to eliminate any remaining divergence associated with terrain height of the grid cell (Goodin et al., 1980).

2.2. Target domains

Two regions in Korea are selected for this study, the Greater Seoul Area (GSA) and the Yochon area. The topography of both areas and the distribution of surface and upper-air meteorology monitoring stations are shown in Fig. 1. GSA is a populated area with about 20 million people, half of the total Korean population. The GSA region has higher topography in the northeast and lower topography in the southwest as shown in Fig. 1. The Yellow Sea is located in the western part of the GSA. High mountains are found in the northeastern part of the GSA where the highest point is 1157 m above sea level (asl). The Yochon area is a basin containing a bay. Yochon is surrounded by hills and mountains; a series of mountains on the northern part of the area are connected to the highest point in the region (1915 m asl).

The entire domain shown in Fig. 1 covers 74×88 grid cells. Each grid cell corresponds to an area of 5×5 km². There are 72 surface meteorology monitoring stations and four upper-air monitoring stations in Korea; 65 of the surface stations and three of the upper-air stations are inside the domain shown in Fig. 1. The GSA covers an area of 38×30 grid cells with 12 surface stations and one upper-air station. The Yochon area covers an area of 20×20 grid cells with five surface stations and one upper-air station in the west. Related to the number and distribution of monitoring stations, two parameters can be defined: station density and radius of influence. The station density, the number of stations per unit area, is

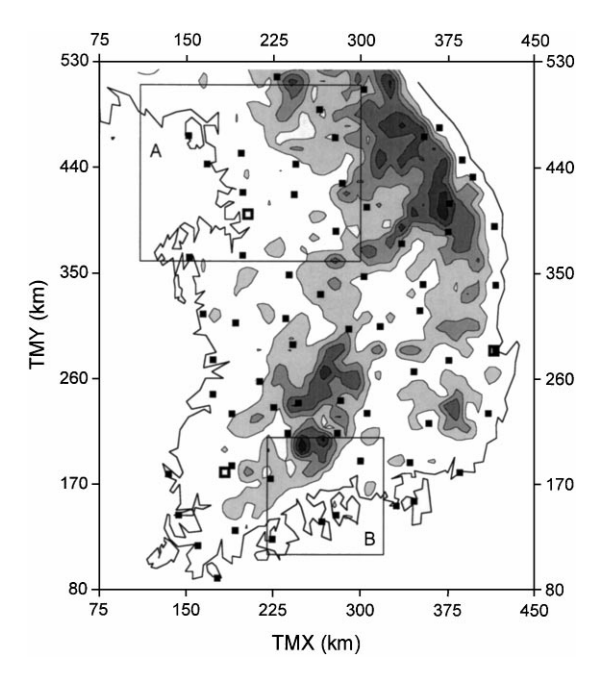


Fig. 1. Topography and distribution of meteorology monitoring stations in the southern part of the Korean Peninsula. Filled contours represent height of topography above sea level starting from 200 m at intervals of 200 m. Solid squares represent the locations of surface meteorology monitoring stations and larger bold open squares represent the locations of upper-air monitoring stations. "A" and "B" indicate the Greater Seoul Area and the Yochon area, respectively, the two test areas in the present paper.

 4.2×10^{-4} km⁻² for GSA and 5.0×10^{-4} km⁻² for the Yochon area. The radius of influence is the distance between a measuring station and the farthest location where the effect of measured data is still "felt". It is an important parameter in the interpolation process, and is calculated as suggested by Stephens and Stitt (1970). In this study the radius of influence is set to 125 km.

2.3. Episode

Throughout the summer of 1994 hot and arid air was stagnant over the Korean Peninsula. Daily maximum temperatures exceeded 30°C on 44 days of July and August. Because of this high temperature, the highest two ozone concentrations of 1994 (322 and 243 ppb) were recorded at the Kwanghwamun monitoring station, located in the middle of Seoul, on August 23 and 24. July was in the middle of the hot summer. In particular, on July 17 one of the highest ozone concentrations (227 ppb) of this summer was measured and eight of the 20 monitoring stations in Seoul reported exceedances of the 1-h ozone standard of 100 ppb. For this day, three-dimensional wind fields were generated on an hourly basis for the two target domains in Fig. 1.

2.4. Convergence parameters

The optimum wind field is determined by increasing the size of the estimation domain over the target domain. By increasing the size of the estimation domain, more data from monitoring stations outside the target domain are used to predict the wind field, but their relative contributions are diminished. Therefore, convergence of the predicted wind field is expected. The degree of convergence of the predicted wind field is determined according to

$$D_{WS}(\text{max}) = [\text{abs}(WS^{(N)} - WS^{(N-1)})/WS^{(N-1)}_{\text{max}}]_{\text{max}},$$

$$D_{WD}(\text{max}) = [\text{abs}(WD^{(N)} - WD^{(N-1)})]_{\text{max}},$$
(1)

where WS is the wind speed, WD the wind direction, and WS_{max} the domain maximum wind speed. The superscripts (N) and (N-1) indicate that the variables are calculated from the current and previous wind field predictions by increasing the domain size. Relative differences are reported for wind speed and absolute differences for wind direction. For both variables, maximum differences are used.

3. Results and discussion

3.1. Measurements vs. predicted wind field

In Fig. 2, predicted wind speeds on the surface of the entire domain of Fig. 1 are compared with the measurements in order to understand the features of estimated wind field by the diagnostic routine. Twenty-four hour data for 65 monitoring stations on July 17, 1994 are presented except the calm cases in which the wind speed was less than 0.3 m/s since these might introduce errors in wind direction calculations. The relationship between measured and calculated wind speeds is good; the squared correlation coefficient, R^2 , has a value of 0.96. In addition, the intercept of the best-fitted line is 0.03 m/s, which is close to zero. However, the slope of the best-fitted line is 0.81 and larger values are underestimated as a result of smoothing of the measurements during the calculation. The smoothing effect of the diagnostic routine shown in this figure is noticeable since it could lower peak ozone concentrations by blurring the sharp variations associated with locally high speed of wind.

The same phenomenon is reported by Kumar and Russel (1996), but they only indicate that meteorological fields generated by the diagnostic approach correlate better with the observed data than those generated by the prognostic approach. Moreover, they show that the photochemical model results obtained from prognostically derived fields exhibit a lower peak for the predicted ozone concentrations than the diagnostic one.

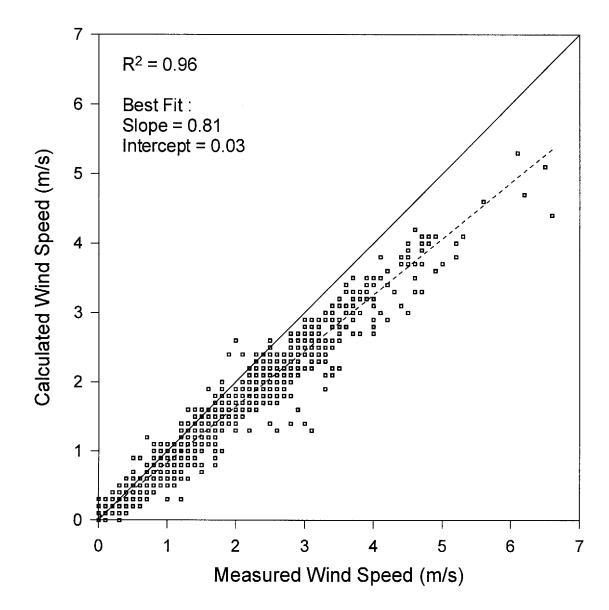


Fig. 2. Scatter diagram of measured and predicted wind speed for surface meteorology monitoring stations in Fig. 1. Dashed line indicates a best fit while the solid line represents a perfect correlation. R^2 is the squared correlation coefficient.

3.2. Convergence test

Convergence test with different sizes of the estimation domain is performed for GSA. A similar procedure is also applied to the Yochon area. Maximum differences according to Eq. (1) are determined from all the wind data calculated for the 24-h period of July 17, 1994 in the target domain. Only surface wind data are used since no additional upper-air stations are available while expanding the estimation domain. The results for GSA are shown in Fig. 3(a). The wind field estimation domain in GSA is increased by 10 km in each direction from the target domain of 190 × 150 km. Differences of both wind speed and wind direction sharply decrease for the first few 10-km increases, and then remain stable after 40 km. During the expansion of the wind field estimation domain, the number of stations increases by 3, 2, 1, 2, 2, 6, 1, etc. every 10 km. Maximum differences are usually observed around the area where stations are added, but the rate of decrease or variation in the difference does not correlate with the added number of stations even in the initial phase of decrease.

Fig. 3(b) shows the results for the Yochon area. The Yochon area is one third the size of GSA, but the station density is slightly higher than that of GSA. By considering the distribution of stations outside the target domain, the estimation domain increases by 10 km for the first two trials, and by 5 km for the next ones. With this expansion, the number of stations increases by 2, 1, 2, 4,

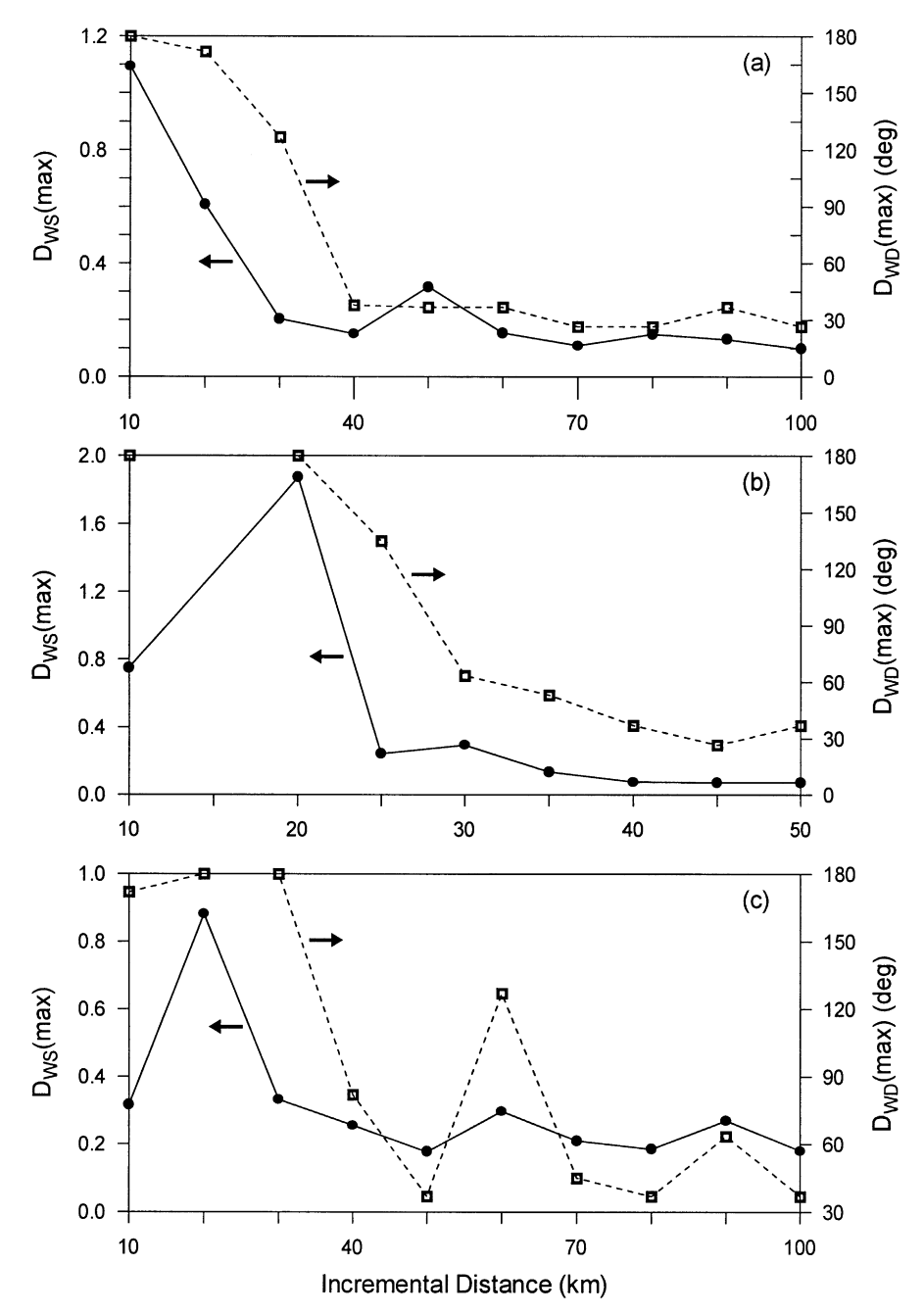


Fig. 3. Variations in maximum differences of wind speed and direction with increasing the estimation domain over the target domain. Solid line is for a maximum difference of wind speed and dashed line for a maximum difference of wind direction. (a) Greater Seoul Area; (b) Yochon area; (c) Greater Seoul Area but with number of stations reduced by a factor of two.

3, 1, 1, etc. Although fluctuations are observed in the initial phase of variations in the wind speed difference, both differences decrease and stabilize after 30 km.

Acceptable levels of $D_{WS}(max)$ and $D_{WD}(max)$ are determined case by case. As shown in Fig. 3(a), 40 km beyond

the target domain is acceptable for GSA. For the Yochon area, 30 km could be a reasonable choice. When these values are chosen, $D_{\rm WS}({\rm max})$ and $D_{\rm WD}({\rm max})$ are 0.15 and 38° for GSA and 0.29 and 63° for the Yochon area, respectively.

Since station densities of GSA and the Yochon area are similar, the effect of the station density cannot be clearly observed in Fig. 3(a) and (b). Therefore, the number of stations in GSA was halved in order to study a case with low station density. As a result of low station density, the radius of influence for each station is slightly increased and set to 150 km. Fig. 3(c) shows the result. The convergence is not smooth, but fluctuations for both wind speed and direction diminish after 70 km, which is about twice the length found for the previous two cases. In spite of several fluctuations, $D_{\rm WS}({\rm max})$ and $D_{\rm WD}({\rm max})$ are 0.21 and 45°, just slightly larger from those of the original GSA. The convergence in the case of low station density shown in Fig. 3(c) will be investigated in more detail subsequently.

3.3. Effects of radius of influence and grid size

Three plots in Fig. 3 show three patterns of convergence: (a) smooth convergence, (b) large fluctuation at first, but then convergence, and (c) continuing fluctuations with decreasing amplitudes. Although an estimation domain 70 km larger than the target domain is suggested for case (c), persistent fluctuations are noticeable. These fluctuations are caused apparently because the station density for Fig. 3(c) is only a half of the previous two cases. In order to find remedies for this unstable situation with fluctuations, the radius of influence and grid size, two important parameters used in the interpolation process, are modified independently. Fig. 4(a) shows the results in which only the radius of influence is modified. It can be seen that the convergence pattern becomes stable as the radius of influence increases. This is interpreted as follows: a larger radius of influence implies that more stations affect a grid point, and consequently, the influence of added stations by increasing the estimation domain becomes smaller relative to the influence of stations within the target domain.

In Fig. 4(b), the grid distance is doubled in length and the results are compared. Doubling the grid distance stabilizes the convergence, and its effect is more pronounced than the previous case when the radius of influence was increased. When doubling the grid distance, the number of grid points is reduced by a factor of four. In the process of enlarging grid distance, sensitive areas that could be affected by added stations are swept, thus maximum differences are reduced.

Fig. 4 shows that both, larger radius of influence and larger grid size, could stabilize the convergence of maximum differences. However, a large radius of influence tends to smooth the estimated wind field in such a way that local variations could be ignored. Furthermore, large grid distance cannot be obtained without a compromise in resolution. After all, optimum size of the estimation domain could be determined in case of sparse distribution of stations, but some smoothing and

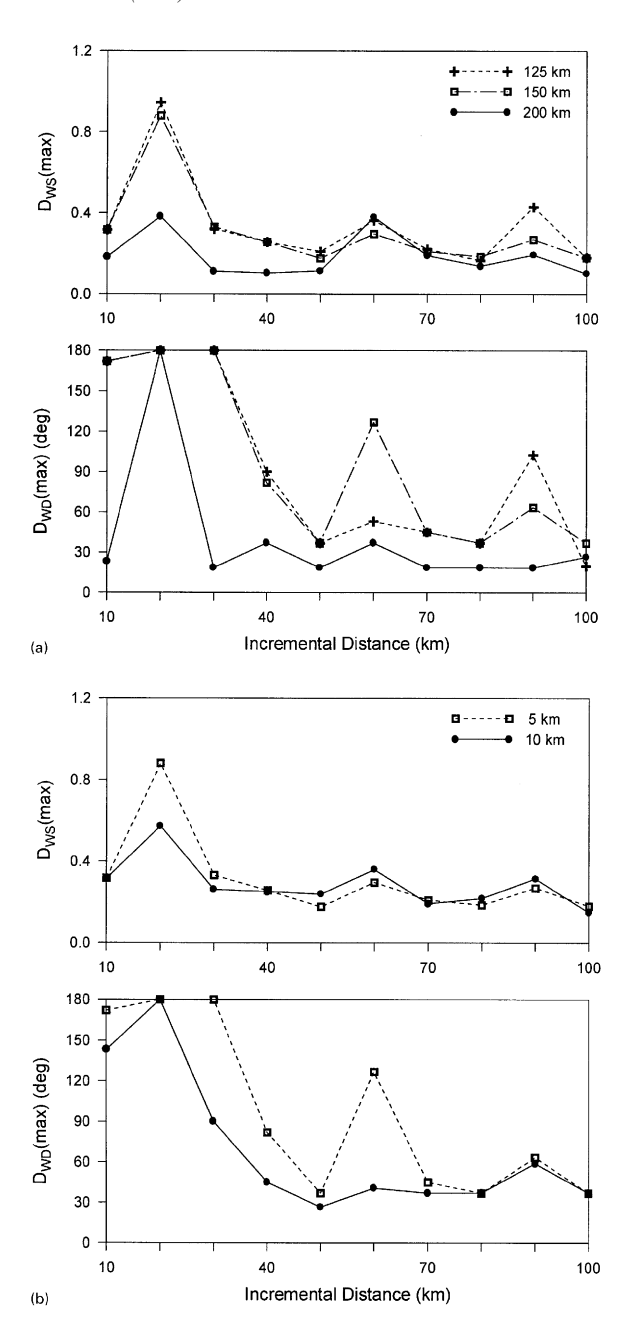


Fig. 4. Variations in maximum differences of wind speed and direction with increasing the estimation domain for the Greater Seoul Area but with number of stations reduced by a factor of two: (a) effects of the radius of influence; (b) effects of grid distance.

decrease in resolution of the estimated wind field would be inevitable.

3.4. Effects of boundary topography

As indicated previously, maximum differences usually occur where stations are added. Nevertheless, Figs. 3

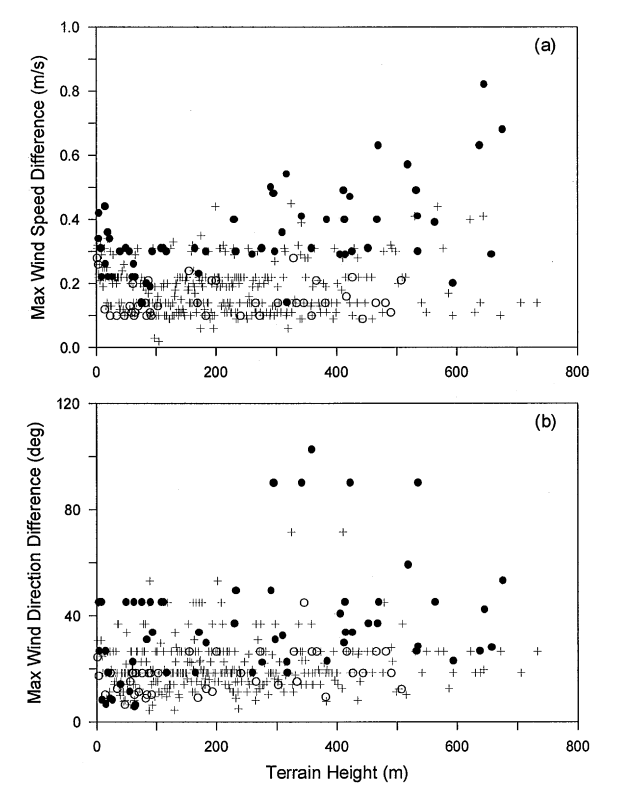


Fig. 5. Maximum differences of wind speed and direction for 24-h data on July 17, 1994 in GSA at each terrain height. Solid circles represent data from east and south boundaries, open circles represent data from west and north boundaries, and crosshairs represent data from the interior grid points: (a) maximum difference of wind speed; (b) maximum difference of wind direction.

and 4 show that differences in both, wind speed and direction, are not decreased below a certain value even with 100 and 50 km incremental distances for GSA and the Yochon area, respectively. The extreme case of increasing incremental distance is to use all the station data available in order to predict the wind field for the target domain. In order to elucidate why maximum differences in Figs. 3 and 4 are sustained even with large incremental distance, the wind data for GSA obtained with 40 km incremental distance as suggested in Fig. 3(a) are compared with those obtained with 65 station data in the entire domain. That is, the estimation domain in the latter case is the entire domain in Fig. 1. Taking into consideration that GSA is a mountainous area and located in the northwest corner of the country, maximum differences of wind speed and direction are calculated from 24-h data of July 17, 1994 at each terrain height by grouping the data into three categories. They are (1) the wind data from the interior area, (2) data from the north and west boundaries beyond which only one or no additional stations are present, and (3) data from the east and south boundaries beyond which there are stations that can be added by expanding the wind field estimation domain.

If there is no differentiation among those categories in the data, a plot of maximum difference of wind speed vs. terrain height would misleadingly show that the largest differences occur where the terrain is complex. Nevertheless, grouping the data into the categories described above shows that for most of the domain there is no correlation between maximum difference of wind speed and topography. Data from east and south boundaries show (1) difference dependence on topography and (2) the largest differences at most topography. On the other hand, differences along the west and north boundaries cannot be distinguished from those of the interior, because the west and north boundaries of GSA are much closer to those of the entire domain as you can see in Fig. 1.

Patterns of variations of wind direction differences shown in Fig. 5(b) are not so clear as those of wind speed differences in Fig. 5(a). The differences along the west and north boundaries cannot be distinguished from those of the interior like the case of wind speed. Nevertheless, large differences along the east and south boundaries are generally observed. In addition, it is interesting to note that the largest difference in Fig. 5(b) is above 100° in spite that the maximum difference of wind direction at 40-km incremental distance is only 38° in Fig. 3(a). This means that the variations in wind direction do not randomly occur and the wind direction varies in one direction in some cases by increasing the wind field estimation domain.

4. Conclusions

A systematic approach to obtain a reliable diagnostic wind field for the target domain is presented. Maximum differences of wind speed and direction are determined for various wind field estimations at appropriate intervals of incremental distance. Two areas in Korea are studied: the Greater Seoul Area (GSA) and the Yochon area. Maximum differences sometimes fluctuate but in general they decrease smoothly to give an optimum size of the estimation domain. Incremental distances to optimum estimation domain over the target domain are 40 km for $190 \times 150 \text{ km}$ of GSA and 30 km for $100 \times 100 \text{ km}$ of the Yochon area.

When the number of station is halved, fluctuations are frequently observed in the variations of maximum differences. Employing both larger radius of influence and grid distance stabilizes the convergence by reducing the influence of additional stations. However, this stabilization is a result from smoothing and the compromise in the resolution of the wind field. An extreme case of increasing incremental distance is to use all station data available to

estimate the wind field of the target domain. When the wind field from a limited estimation domain is compared with that from all available station data, large differences usually occur along boundaries beyond which there are additional stations present and where the terrain is high. The former is inevitable as long as a limited size of domain and a limited number of stations are employed. Nevertheless, the latter would be alleviated if the complex terrain on the boundary is avoided.

Acknowledgements

This work was supported by the Korea Institute of Science and Technology and partly also by a grant from the IBM Environmental Research Program. Any opinions, findings and conclusions or recommendations expressed in this material are those of the authors and do not necessarily reflect the views of the IBM Corporation.

References

- Goodin, W.R., McRae, G.J., Seinfeld, J.H., 1980. An objective analysis technique for constructing three-dimensional urban-scale wind fields. Journal of Applied Meteorology 19, 98–108.
- Harley, R.A., Russel, A.G., McRae, G.J., Cass, G.R., Seinfeld, J.H., 1993. Photochemical modeling of the Southern California air quality study. Environmental Science and Technology 27, 378–388.
- Kumar, N., Russell, A.G., 1996. Comparing prognostic and diagnostic meteorological fields and their impacts on photochemical air quality modeling. Atmospheric Environment 30, 1989–2010.
- Seinfeld, J.H., 1988. Ozone air quality models. A critical review. Journal of Air Pollution Research Association 38, 616–645.
- Solomon, P.A., 1995. Regional photochemical measurement and modeling studies: a summary of the air and waste management association international specialty conference. Journal of Air and Waste Management Association 45, 253–286.
- Stephens, J.J., Stitt, J.M., 1970. Optimum influence radii for interpolation with the method of successive corrections. Monthly Weather Review 98, 680-687.